IMPROVEMENT OF THE REYNOLDS-STRESS MODEL BY A NEW PRESSURE-STRAIN CORRELATION

by
Ryoichi S. Amano - Principal Investigator
and
John C. Chai - Research Assistant

Department of Mechanical Enigineering
University of Wisconsin-Milwaukee
Milwaukee, Wisconsin 53201

Status Report

April 1988

The report documents research completed during the period of January 1988 through April 1988 under NASA-Marshall Space Flight Center Grant No. NAG 8-617

ABSTRACT

A study is made to improve the predictions of Reynolds stresses in a backward facing step flows, through modifications of the pressure-strain correlation. The mean-strain term of the pressure-strain correlation is formulated only in terms of non-isotropic turbulence in order to take the severe non-isotropic effect caused by a separating flow. This model is compared with other existing models and results are verified with existing experimental results.

TABLE OF CONTENTS

NOMENCLATURE

C_{ϕ_1}, C_{ϕ_2}	pressure strain correlation constants
G	generation rate of turbulent kinetic energy
G_{ij}	generation rate of Reynolds stresses $< u_i u_j >$
H	step height
H_{ij}	secondary generation rate of Reynolds stresses $< u_i u_j >$
k	turbulent kinetic energy
p	fluctuating pressure
Re	Reynolds number based on step height, H
S_{ij}	Surface integral
u	fluctuating velocity in x direction
U	mean velocity in x direction
v	fluctuating velocity in y direction
x,y	Cartesian coordinates

Greek Symbols

α, β	constants in Π_{lj}^{mi}
δ_{ij}	Kronecker delta
ϵ	dissipation rate of turbulent kinetic energy
$\phi_{ij,1}, \phi_{ij,2}$	pressure-strain correlations for Reynolds stresses
Π_{lj}^{mi}	fourth-order tensor
ρ	density of fluid
ν	kinematic viscosity

Subscripts/Superscripts

i,j,k,l,m,n	tensor notations

Symbols

$\langle\rangle$	time-averaged values

1 INTRODUCTION

Separation and recirculation of flow is a common flow phenomena in many industrial problems. It associates itself with higher turbulence levels which not only render the flow greater analytical complexity but also result in highly augmented heat and momentum transfer. Therefore, mathematical models that can predict complex turbulent flows are needed. It has been commonly accepted that any isotropic turbulence models such as the $k - \epsilon$ model et al. cannot take the non-isotropic effect into account in the evaluation of turbulence levels, whereas this effect is significant in complex turbulent flows. This is why the presents authors have been investigating to establishing a turbulence model based on the Reynolds stresses. The pressure-strain correlation term of the Reynolds-stress equations can be divided into two parts: the turbulence term and the mean strain term. The turbulence term controls the energy exchange between the normal stress components in relatively smaller eddies and the latter does the same in larger eddies. Our main focus is the evaluation of stresses in large eddies through the separating and reattaching flow which suffers strong curvature effect from the recirculation of flow.

In improving the computations of the Reynolds stresses, the authors discovered that the closure models of the mean strain term of the pressure-strain correlation significantly affects the results in the separating and reattaching flows.

The model for the turbulence term in the pressure-strain correlation was developed by Rotta [1] and it has given effectively reasonable results with the anisotropy form. However, the existing models for mean strain term of the pressure-strain correlation proposed by several researchers [2-4] do not reach to a compromizing level in the computation of such a separating flow with recirculation. Thus, the authors have established a tensor that does not contain any terms which have isotropic turbulence but have only quantities with non-isotropic turbulence. The new model was compared with the existing models mentioned above. All models were then compared with experimental results of Chandrsuda and Bradshaw [5] with Reynolds number of 10^5.

Since constants of the existing models were determined by comparing with plane homogeneous shear flows [4], modifications were made for re-

circulating and separating flows through analytic comparison with experimental values , and computer optimazations.

2 MATHEMATICAL MODELS

2.1 Governing Equations

The set of differential equations governing the transport of the kinematic Reynolds stresses ,$< u_i u_j >$ can be written in the form :

$$\frac{\partial}{\partial x_j}(U_j < u_i u_j >) = -\left[< u_j u_k > \frac{\partial U_i}{\partial x_k} + < u_i u_k > \frac{\partial U_j}{\partial x_k}\right] - 2\nu < \frac{\partial u_i}{\partial x_k}\frac{\partial u_j}{\partial x_k} >$$
$$-\nu\left(< \frac{\partial u_k}{\partial x_i}\frac{\partial u_j}{\partial x_k} > + < \frac{\partial u_k}{\partial x_j}\frac{\partial u_i}{\partial x_k} >\right) + < \frac{p}{\rho}\left(\frac{\partial u_j}{\partial x_i} + \frac{\partial u_i}{\partial x_j}\right) >$$
$$-\frac{\partial}{\partial x_k}\left[< u_i u_j u_k > + \frac{< u_i p >}{\rho}\delta_{jk} + \frac{< u_j p >}{\rho}\delta_{ik}\right]$$
$$-\nu\left(\frac{\partial}{\partial x_k} < u_i u_j > + < u_j \frac{\partial u_k}{\partial x_i} > + < u_i \frac{\partial u_k}{\partial x_j} >\right) \quad (1)$$

To close eq. (1) in terms of mean velocities and the Reynolds stresses, the turbulence quantities on the right-hand side of eq. (1) must be represented by empirical functions of mean velocities, the Reynolds stresses and their derivatives.

In this study, attention was focused on the approximation of the fourth group of terms of the right-hand side of eq. (1), namely the "pressure-strain correlation". The rate of the "pressure-strain correlation" is the redistributive effect ; thus, this correlation mainly controls the energy distribution.

The authors have tested several models of the pressure-strain correlation and discovered that it was necessary to remodel this correlation for the computations of flows which are accompanied by flow recirculation. Some existing models are summarized in the next subsection.

2.2 Summary of Existing Models

Generally, the pressure-strain correlation is divided into two parts: one with turbulence effect only and the other with both turbulence and the

mean strain rates. The first part with the turbulence effect was formulated by Rotta [1] in the form of anisotropy which is represented by the symbol $\phi_{ij,1}$ and the last term has been proposed in several ways as follows :

Model 1 : Naot et al. [2]

$$< \frac{p}{\rho}\left(\frac{\partial u_i}{\partial x_j} + \frac{\partial u_j}{\partial x_i}\right) >= -C_{\phi_2}(G_{ij} - \frac{2}{3}\delta_{ij}G) + \phi_{ij,1} \tag{2}$$

Model 2 : Launder et al. [4]

$$< \frac{p}{\rho}\left(\frac{\partial u_i}{\partial x_j} + \frac{\partial u_j}{\partial x_i}\right) >= -\frac{(C_{\phi_2}+8)}{11}(G_{ij} - \frac{2}{3}\delta_{ij}G)$$

$$-\frac{(30C_{\phi_2}-2)}{55}k\left(\frac{\partial U_i}{\partial x_j} + \frac{\partial U_j}{\partial x_i}\right) - \frac{(8C_{\phi_2}-2)}{11}(H_{ij} - \frac{2}{3}\delta_{ij}G) + \phi_{ij,1} \tag{3}$$

where

$$G = - < u_i u_j > \frac{\partial U_i}{\partial x_j} \tag{4}$$

$$G_{ij} = -\left(< u_i u_k > \frac{\partial U_j}{\partial x_k} + < u_j u_k > \frac{\partial U_i}{\partial x_k}\right) \tag{5}$$

$$H_{ij} = -\left(< u_i u_k > \frac{\partial U_k}{\partial x_j} + < u_j u_k > \frac{\partial U_k}{\partial x_i}\right) \tag{6}$$

$$\phi_{ij,1} = -C_{\phi_1}\frac{\epsilon}{k}\left(< u_i u_j > -\frac{2}{3}\delta_{ij}k\right) \tag{7}$$

The first model was developed by removing the isotropic constraint from the double-velocity, two-point correlation tensor. The second model was obtained by approximating the pressure-strain correlation by an arbitrary fourth-order tensor, where the single-point correlation was used.

The value of C_{ϕ_1} was set equal to 1.5, and through computer optimizations, C_{ϕ_2} was recommended to be 0.7 and 0.4 for model of Naot and Launder respectively.

2.3 Formulation of A New Model

Following Chou [6], a Poisson equation for the fluctuating pressure, p, can be obtained by taking the divergence of the equation for the fluctuating velocity u_i, which can be re-expressed to write the pressure-strain correlation as

$$< \frac{p}{\rho}\frac{\partial u_i}{\partial x_j} >= S_{ij} +$$

$$\frac{1}{4\pi}\int_{vol}\left[< \left(\frac{\partial^2 u_l u_m}{\partial x_l \partial x_m}\right)' \frac{\partial u_i}{\partial x_j} > +2\left(\frac{\partial U_l}{\partial x_m}\right)' < \left(\frac{\partial u_m}{\partial x_l}\right)' \left(\frac{\partial u_i}{\partial x_j}\right) >\right] \frac{d\,vol}{x-y} \quad (8)$$

where the first and second terms in the integral are denoted as $\phi_{ij,1}$ and $\phi_{ij,2}$ respectively, and S_{ij} is a surface integral which is negligible away from a solid wall.

Following Rotta's proposal [1], $\phi_{ij,1}$ was formulated same as one given by eq. (7) with $C_{\phi_1} = 1.5$. Furthermore, $\phi_{ij,2}$ may be approximated as

$$\phi_{ij,2} = \frac{\partial U_l}{\partial x_m}\Pi_{lj}^{mi} \quad (9)$$

where Π_{lj}^{mi} is a fourth-order tensor which satisfies the kinematic constraints of

$$\Pi_{lj}^{mi} = \Pi_{lj}^{im} = \Pi_{jl}^{im} \quad (10)$$

$$\Pi_{li}^{mi} = 0 \quad (11)$$

$$\Pi_{jj}^{mi} = 2 < u_m u_i > \quad (12)$$

Equation (12) suggests that Π_{jj}^{mi} can be approximated by a linear combination of the Reynolds stresses. On neglecting isotropy effects, the tensor can be expressed as :

$$\Pi_{lj}^{mi} = \alpha\delta_{lj} < u_m u_i > +\beta(\delta_{ml} < u_i u_j > +\delta_{mj} < u_i u_l >$$

$$+\delta_{il} < u_m u_j > +\delta_{ij} < u_m u_l >) + C_{\phi_2}\delta_{mi} < u_l u_j > \quad (13)$$

where the condition of eq. (10) is already imposed. The application of eqs. (11), and (12) enables two of these constants to be expressed in terms of the third, namely C_{ϕ_2} and can be written as

$$\alpha = C_{\phi_2} + 1$$

$$\beta = C_{\phi_2}$$

The final form is given as

$$< \frac{p}{\rho}\left(\frac{\partial u_i}{\partial x_j} + \frac{\partial u_j}{\partial x_i}\right) >= -(2C_{\phi_2} + 1)(G_{ij} - \frac{2}{3}\delta_{ij}G)$$

$$-2C_{\phi_2}(H_{ij} - \frac{2}{3}\delta_{ij}G) - \frac{(14C_{\phi_2} + 2)}{3}\delta_{ij}G \quad (14)$$

The coefficient C_{ϕ_2} can be determined by simplifying the Reynolds stresses described by eq. (1) into an algebraic equation which was originally developed by Rodi [7].

If the convection-diffusion string of the $< u_i u_j >$ is set to be equal to that of the turbulence kinetic energy, k, it follows that,

$$\frac{\partial}{\partial x_j}(U_j < u_i u_j >) - D_{ij} = \frac{< u_i u_j >}{k}\left[\frac{\partial}{\partial x_j}(U_j k) - D_k\right] \quad (15)$$

where D_{ij} and D_k denote, respectively, the diffusion rates of $< u_i u_j >$ and k. After some manipulation, eq. (15) can be re-arranged into the following form,

$$\left(< u_i u_j > -\frac{2}{3}\delta_{ij}k\right)\frac{1}{k} = -\frac{1}{C_{\phi_1}\epsilon}\frac{2}{3}\delta_{ij}G$$

$$-\left[\frac{2C_{\phi_2}(G_{ij} + \frac{1}{2}\delta_{ij}G) + 2C_{\phi_2}(H_{ij} + \frac{1}{2}\delta_{ij}G)}{C_{\phi_1}\epsilon}\right] \quad (16)$$

By assuming that the dissipative action is isotropic, and the flow is parabolic, eq. (16) can be further reduced to :

$$\left(< uu > -\frac{2}{3}k\right)\frac{1}{k} = -\frac{(6C_{\phi_2} + \frac{2}{3})}{C_{\phi_1}} \tag{17}$$

$$\left(< vv > -\frac{2}{3}k\right)\frac{1}{k} = -\frac{(6C_{\phi_2} + \frac{2}{3})}{C_{\phi_1}} \tag{18}$$

$$\left(< ww > -\frac{2}{3}k\right)\frac{1}{k} = -\frac{(2C_{\phi_2} + \frac{2}{3})}{C_{\phi_1}} \tag{19}$$

The above set of relations are compared with typical experimental data for several parabolic flows, and the coefficient C_{ϕ_2} is found as;

$$C_{\phi_2} = -\frac{1}{5}$$

Further investigations through comparison with recirculating flows, it was concluded that

$$C_{\phi_2} = -\frac{1}{10}$$

is the optimum value for prediction of separating and recirculating flows.

3 NUMERICAL METHOD

3.1 Numerical Procedure

Formulation and discretization of all transport equations were performed by using the conventional control-volume approach of Patankar [8],by breaking each equation into diffusion, convection, and source terms. The system of equations were made linear so that they could be solved iteratively by the tridiagonal matrix algorithm. The convection-diffusion string was evaluated through the fourth-order approximation of the exponential form [9]. After several numerical tests, it was observed that the variation in results of

skin friction coefficient, pressure coefficient and mean velocity lie within 2% when the grid is changed from 52 x 52 to 62 x 62. Therefore the grid independent state was assumed to be attained with the grid of 62 x 62 [10].

Computations are performed by using a variable grid mesh with the grid expanding linearly at the rate of 2% in the axial direction and at 3% in the transverse direction from the step wall. The iterative procedure is terminated when the maximum value of the relative residual sources of U, V, and mass balance falls below 1%, which is often achieved with 1000 iterations.

The complete process of solving the momentum, turbulent kinetic energy and the Reynolds stresses takes about 60 minutes of CPU time on a UNIVAC 1100 computer.

3.2 Boundary Conditions

At the inflow, outflow, and symmetry axis, conventional conditions are employed; prescribed values are provided at the inflow region, and zero gradients of the variable are used at the outflow region and the symmetry axis.

At the wall boundary the wall function treatment is employed for the momentum and the turbulent kinetic energy. The dissipation rate is evaluated under the local equilibrium condition. Details of these conditions are given in [11]. The wall boundary conditions of the Reynolds stresses are as follow:

$$- < uv >= -0.238k + \frac{y}{\rho}\frac{dp}{dx} \tag{20}$$

$$< uu >= 1.214k \tag{21}$$

$$< vv >= 0.238k \tag{22}$$

The above equations are used for the grids adjacent to a solid wall.

4 DISCUSSION OF RESULTS

Figure 1 depicts the flow geometry and numerical grid used in the present computations. The height of the channel is magnified five times for better visualization.

Figure 2 shows the velocity variations inside the solution domain. It can be seen that shear flow separates at the edge of the step and forms a separating shear layer which causes a part of the fluid to recirculate in the region confined by a step and the bottom wall, and the rest to continue to flow downstream contributing to the stabilization of the flow through the formation of a boundary layer in the redeveloping region.

Figures 3 and 4 compare the mean velocity profiles predicted by all three models at two different streamwise locations. It can be seen that the mean velocity is fairly independent of the choice of pressure-strain correlation.

Figures 5 and 6 show the predicted shear stress. Generally all three models overpredicted the levels of the shear stress but the new model improved the prediction in the separating shear layer giving levels closer to the experimental data , whereas models by Naot et al. [2] and by Launder et al.[4] give levels of the Reynolds shear stress nearly zero.

Figures 7 and 8 compare the $< uu >$ profile. Although both models by Naot et al. and by Launder et al. give reasonable results, the agreement with the measured values in the separating shear layer is not quite satisfactory. The new model predicts well in this region but underpredicts at the wall.

Figures 9 and 10 show the $< vv >$ profile. The new model is far more superior than the other two models in predicting this Reynolds stress component in the separating shear layer, but does suffer from overprediction near the wall.

5 CONCLUSIONS

From the above results, it is clear that the development of a new pressure-strain correlation is essential to improve the prediction of the Reynolds stresses particularly in the separating shear layer. A near wall correction might be helpful to improve the prediction near the solid wall.

As mentioned before, the constants C_{ϕ_1} and C_{ϕ_2} might need further modifications to improve the predictions of Reynolds stresses.

REFERENCES

1. J. C. Rotta, Statistische Thearie Nichthomogener Trubulenz, *Z. Phys.*, vol. 129, p.547, 1951.
2. D. Naot, A. Shavit, and M. Wolfshtein, Interaction between Components of the turbulent Velocity Correlation Tensor, *Isr. J. Technol.*, vol 8, p259, 1970.
3. D. Naot, A. Shavit, and M. Wolfshtein, Two-point Correlation Model and the Redistribution of Reynolds Stress, *The Physics of Fluids.*, vol. 16, no. 6, pp.738-743, 1973.
4. B. E. Launder, G. J. Reece, and W. Rodi, Progress in the Development of a Reynolds-Stress Turbulence Closure, *J. Fluid Mech.*, vol. 68, pt. 3, pp. 537-566,1975.
5. C. Chandrsuda, and P. Bradshaw, Turbulence Structure of a Reattaching Mixing Layer, *J. Fluid Mech.*, vol. 110, pp. 171-194, 1981.
6. P. Y. Chou, On velocity correlations and the solutions of the equations of turbulent fluctuation, *Quart. Appl. Math.*, vol. 3, p. 38, 1945.
7. W. Rodi, The Prediction of Free Turbulent Boundary Layers by use of a Two-Equation Model of Turbulence, Ph.D. Thesis, University of London, 1972.
8. S. V. Patankar, *Numerical Heat Transfer and Fluid Flow,* Hemisphere, Washington, D. C., 1980.
9. R. S. Amano, Development of a Turbulence Near-Wall Model and Its Application To Separated and Reattached Flows, *Numerical Heat Transfer*, vol. 7, pp. 59-75, 1984.
10. R. S. Amano, and J. C. Chai, Closure Models of Turbulent Third-Order Momentum and Temperature Fluctuations, *NASA-CR-180421*, Oct 1987.
11. R. S. Amano, and P. Goel, Computations of Turbulent Flow Beyond Backward-Facing Steps Using Reynolds-Stress Closure, *AIAA Journal*, vol.23, no. 9, pp. 1356-1362, 1985.

FIGURE CAPTIONS

Figure 1 Typical grid system used (5:1 magnification radially).

Figure 2 Velocity vectors inside the solution domain.

Figure 3 Mean velocity profile at $\frac{x}{H} = 5.4$

Figure 4 Mean velocity profile at $\frac{x}{H} = 6.4$

Figure 5 $< uv >$ profile at $\frac{x}{H} = 8.4$

Figure 6 $< uv >$ profile at $\frac{x}{H} = 10.3$

Figure 7 $< uu >$ profile at $\frac{x}{H} = 8.4$

Figure 8 $< uu >$ profile at $\frac{x}{H} = 10.3$

Figure 9 $< vv >$ profile at $\frac{x}{H} = 8.4$

Figure 10 $< vv >$ profile at $\frac{x}{H} = 10.3$

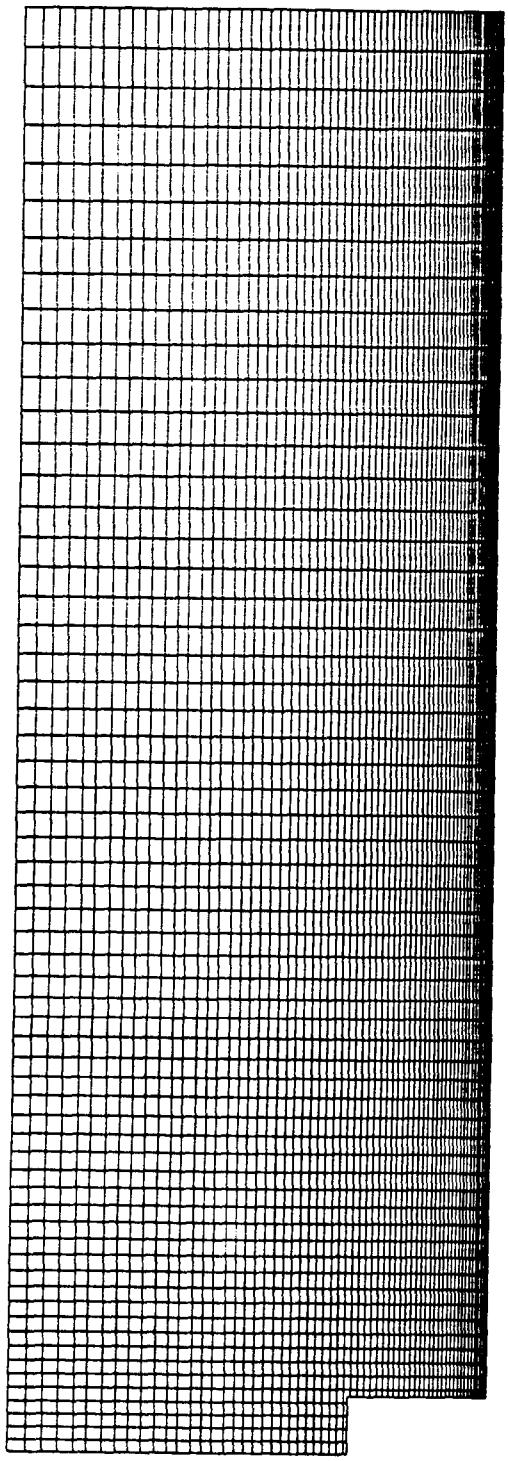

Figure 1 Typical grid system used (5:1 magnification radially).

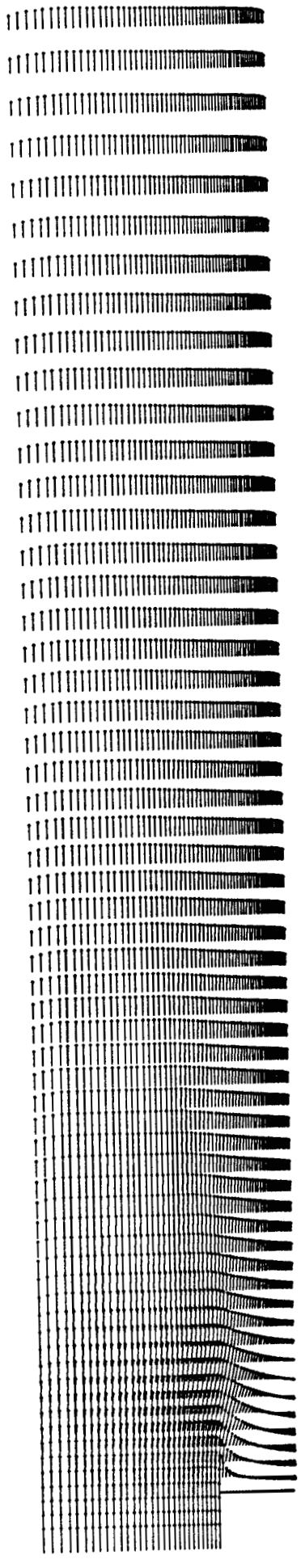

Figure 2 Velocity vectors inside the solution domain.

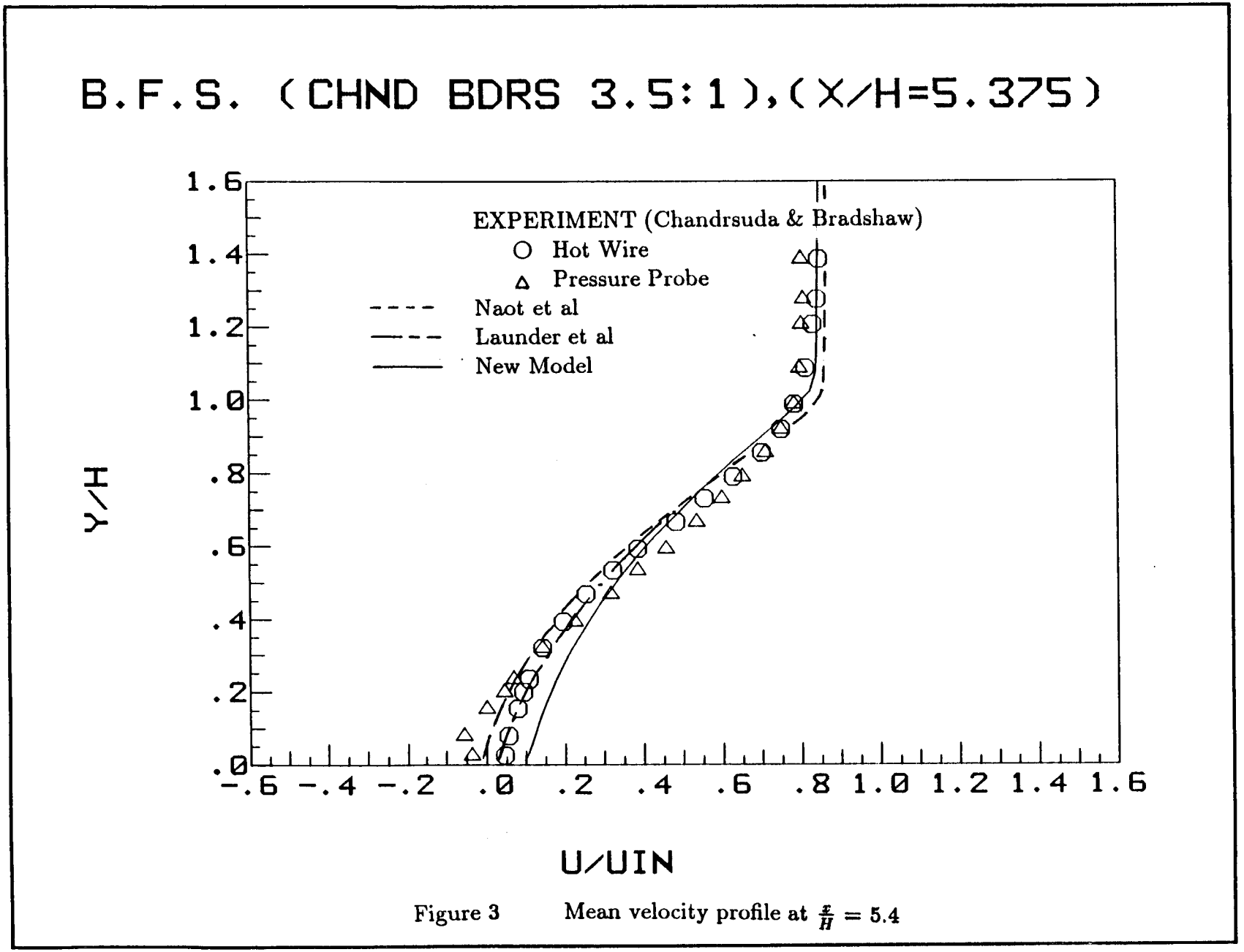

Figure 3 Mean velocity profile at $\frac{x}{H} = 5.4$

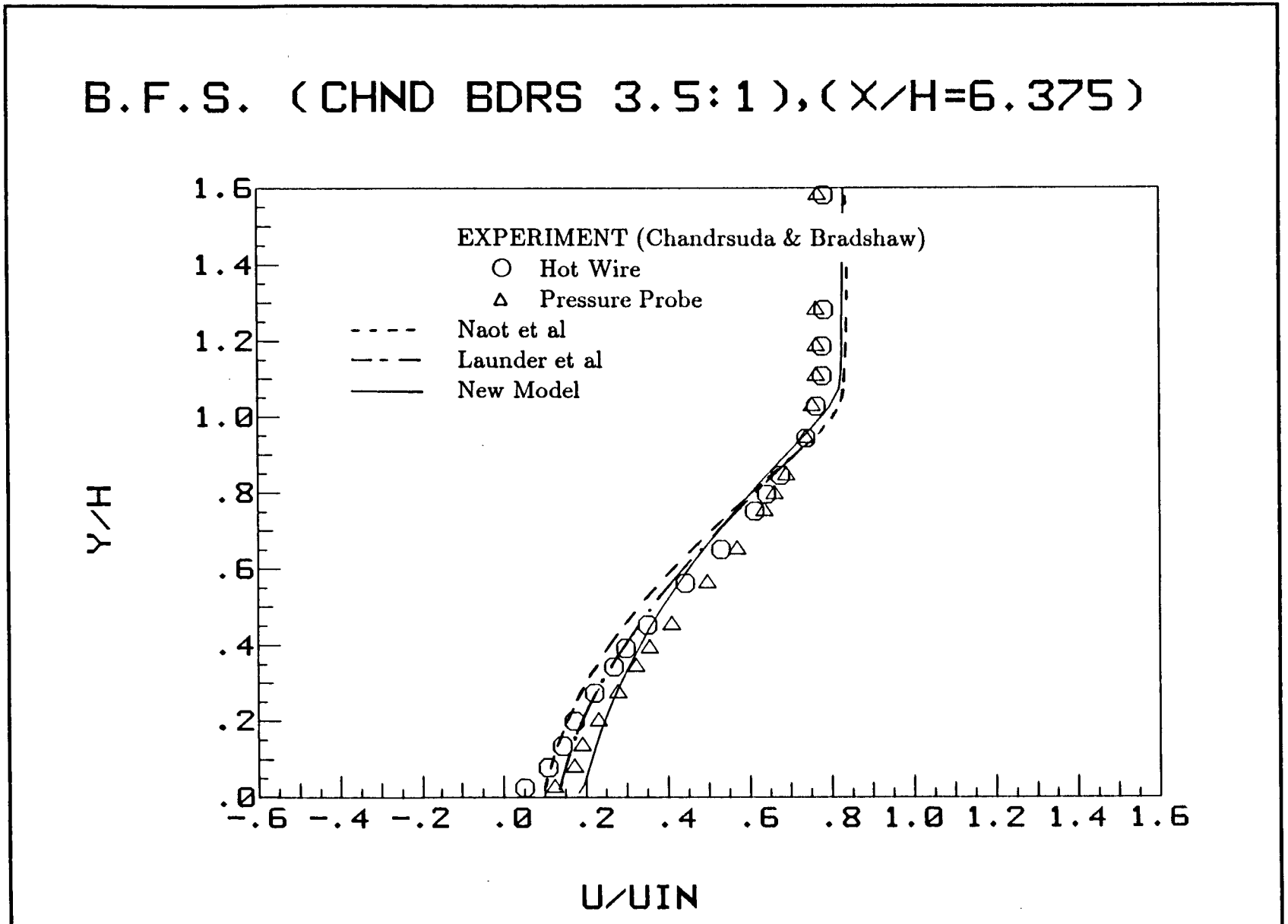

Figure 4 Mean velocity profile at $\frac{x}{H} = 6.4$

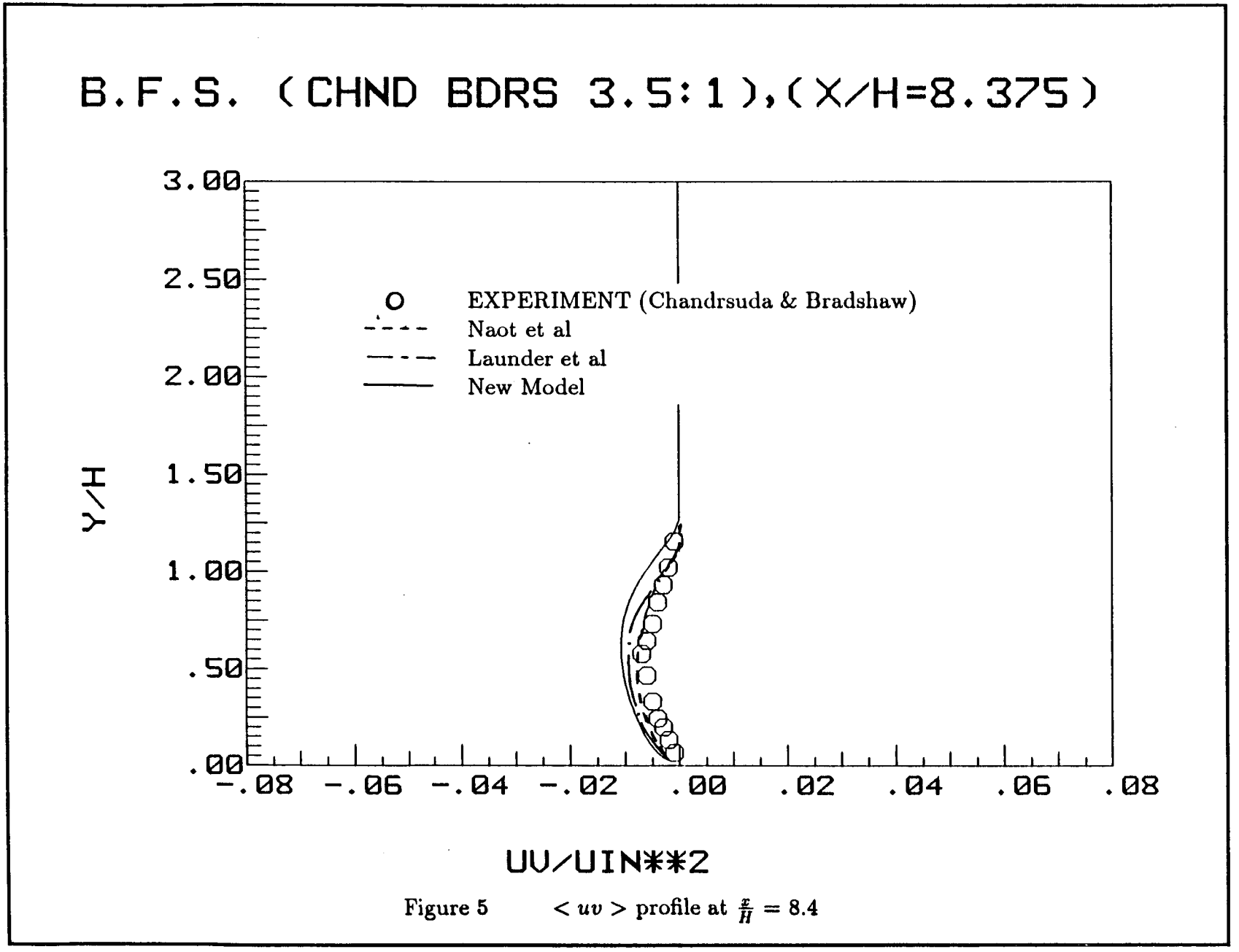

Figure 5 $< uv >$ profile at $\frac{x}{H} = 8.4$

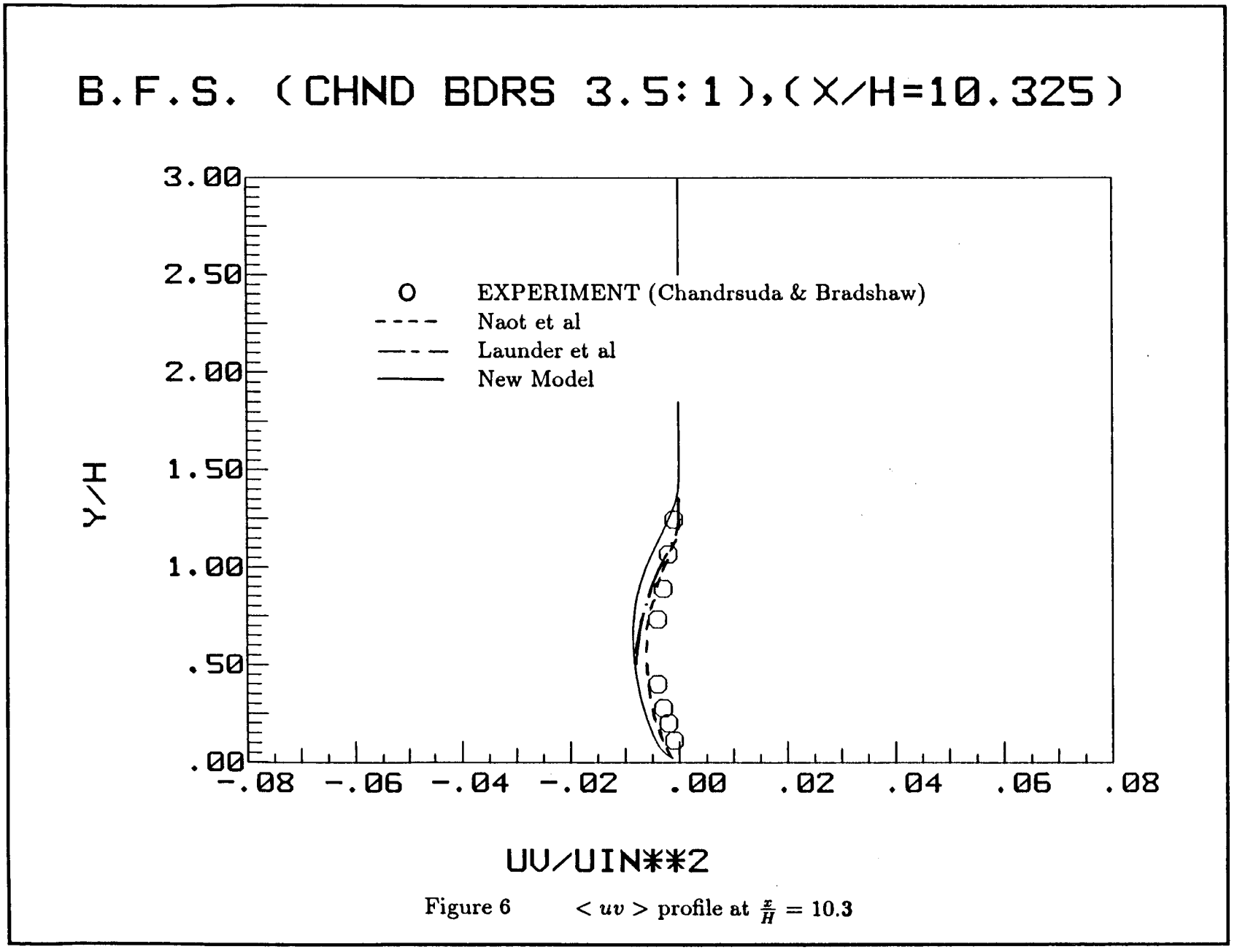

Figure 6 $< uv >$ profile at $\frac{x}{H} = 10.3$

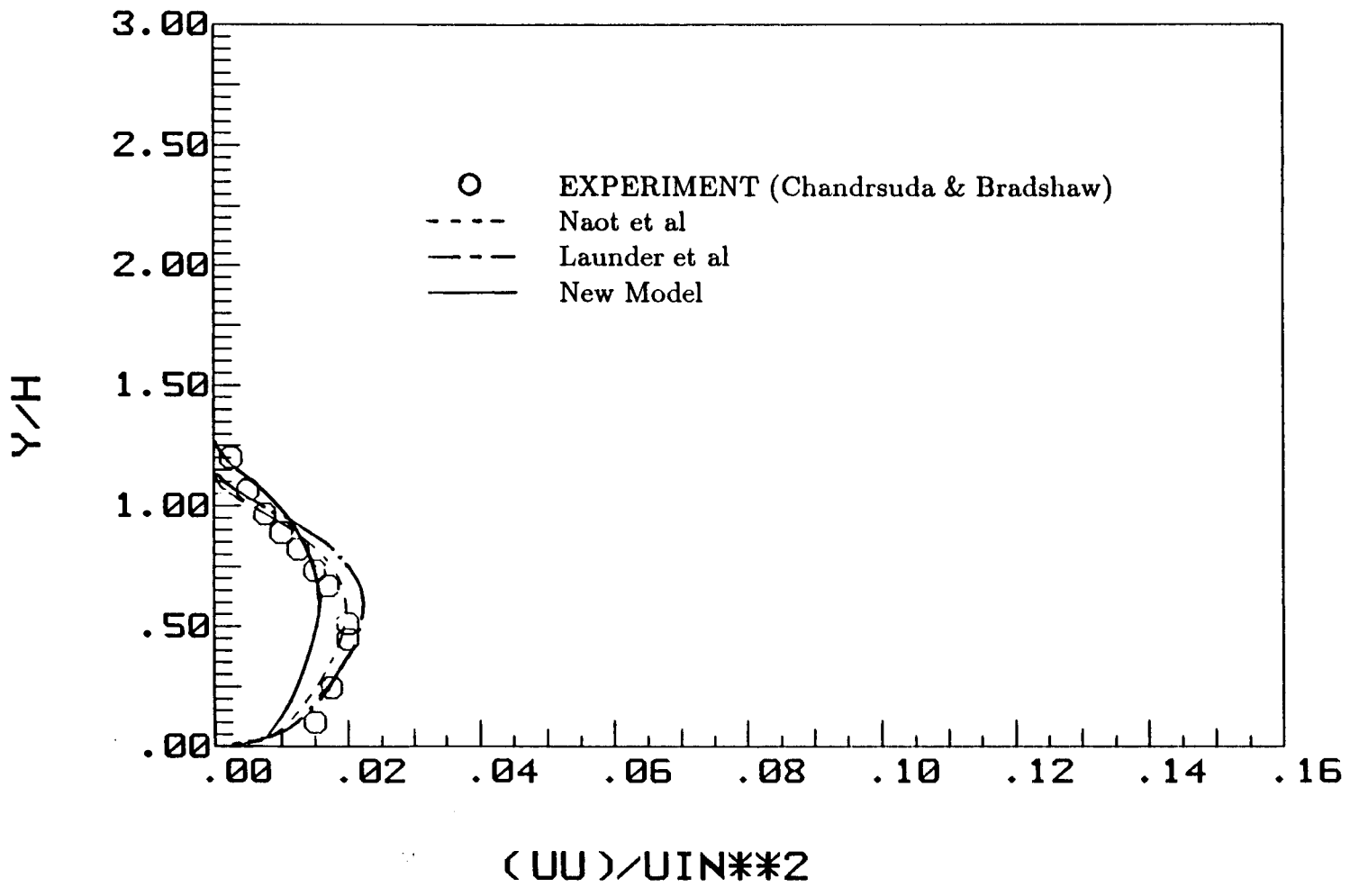

Figure 7 $< uu >$ profile at $\frac{x}{H} = 8.4$

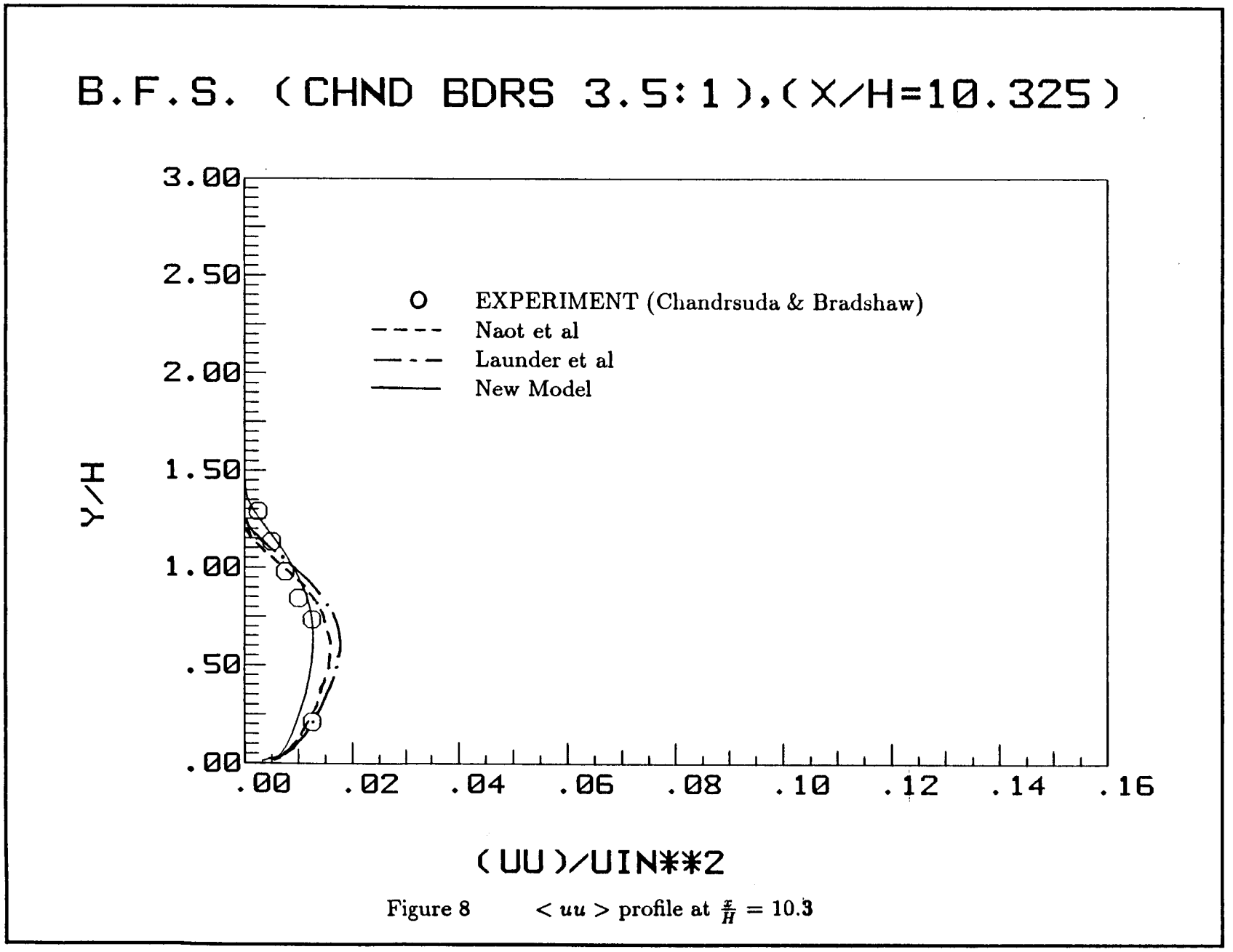

Figure 8 $< uu >$ profile at $\frac{x}{H} = 10.3$

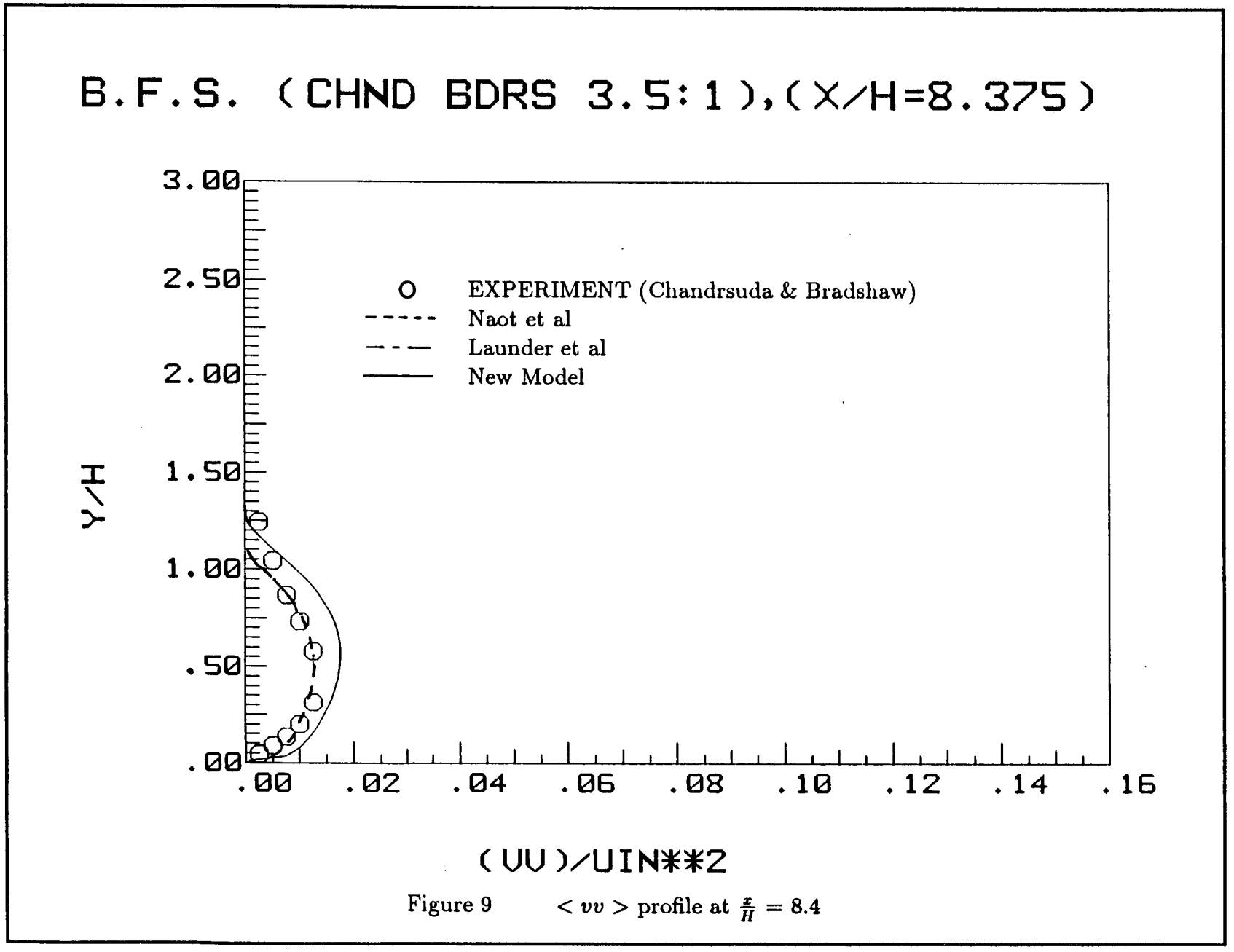

Figure 9 $< vv >$ profile at $\frac{x}{H} = 8.4$

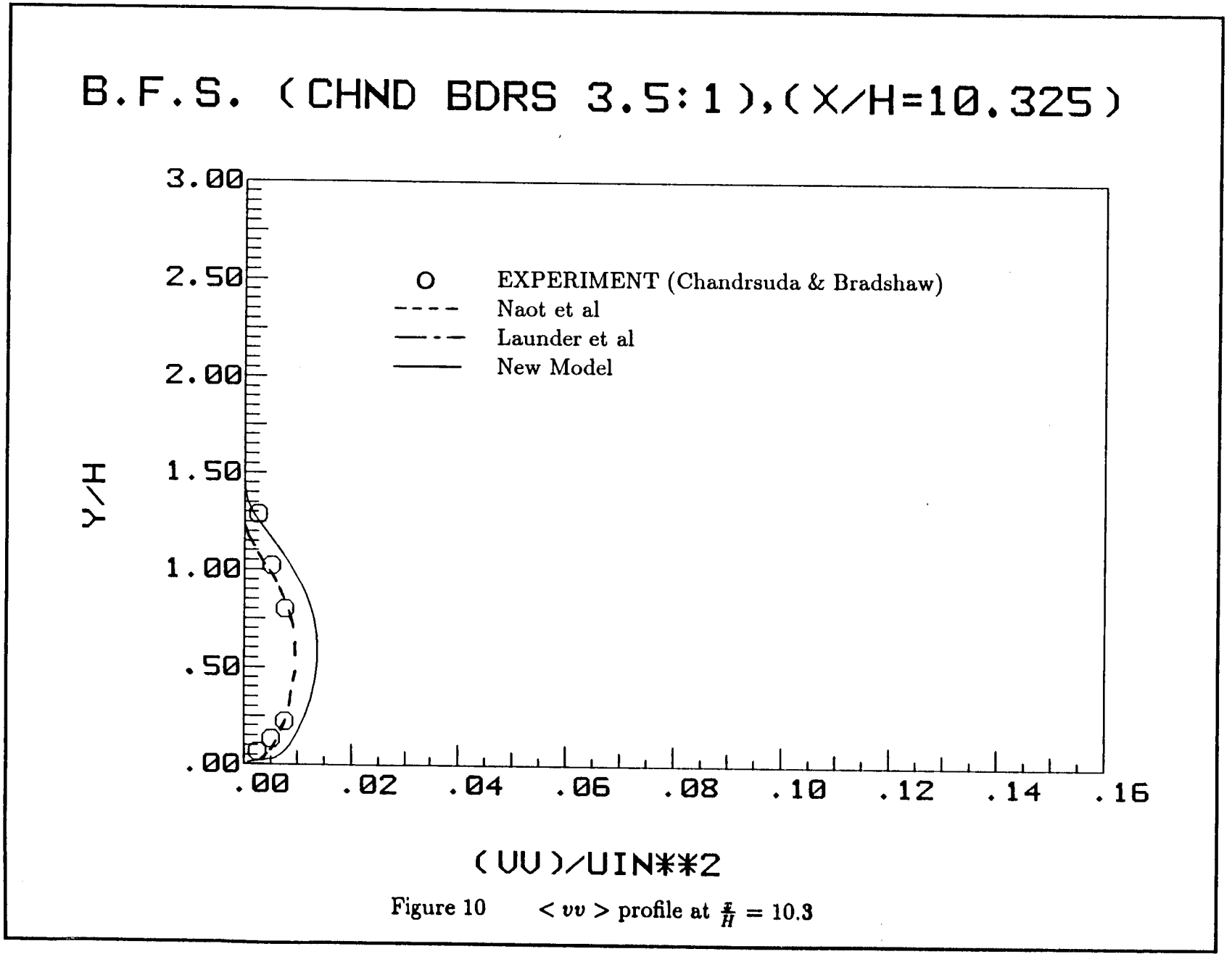

Figure 10 $< vv >$ profile at $\frac{x}{H} = 10.3$